FIG. 1: Sketch of the setup: M stands for mirrors and B for balanced beam-splitters. A non-degenerate parametric amplifier (down-converter DC) generates two-mode squeezed vacuum in modes $\hat{a}_1$ and $\hat{b}_1$. These are fed into an interferometer, with a phase shifter Φ; its output modes $\hat{a}_3$ and $\hat{b}_3$ are detected by homodyne detectors H_a and H_b whose signals are multiplied. Note, that neither the amplifier's pump-laser nor the laser for homodyne detection is shown, also, typically, the polarization of modes $\hat{a}_1$ and $\hat{b}_1$ does not conform and has to be adjusted.

The use of balanced homodyne detection removes the detection problems mentioned above. Because only well established technology is required [18, 19, 20] a proof-of-principle experiment will be immediately possible.

In order to derive our main result (1) we follow the conventions of reference [21]: In the Heisenberg picture the action of the parametric amplifier is described by photon operator transformations $\hat{a}_1 = U\hat{a}_0 + V\hat{b}_0^\dagger$ and $\hat{b}_1 = U\hat{b}_0 + V\hat{a}_0^\dagger$ where $U = \cosh G$ and $V = -i\exp(i\xi)\sinh G$ with the single pass gain $G = g|E_p|L$ and a relative phase ξ which we will assume to be zero. L is the interaction path length, E_p the pump laser's amplitude, and g the gain coefficient proportional to the nonlinear susceptibility $\chi^{(2)}$ of the down-conversion medium DC. Beam splitter B_1 is described by $\hat{a}_2 = \exp(i\Phi)(\hat{a}_1 - i\hat{b}_1)/\sqrt{2}$ and $\hat{b}_2 = (-i\hat{a}_1 + \hat{b}_1)/\sqrt{2}$; note that the interferometric phase shift Φ in arm $\hat{a}_2$ is included. The action of the beam mixer B_2 is analogously described by $\hat{a}_3 = -(\hat{a}_2 - i\hat{b}_2)/\sqrt{2}$ and $\hat{b}_3 = (-i\hat{a}_2 + \hat{b}_2)/\sqrt{2}$ and the total transformation thus reads

$$\hat{a}_3 = \frac{1-e^{i\Phi}}{2}(U\hat{a}_0 + V\hat{b}_0^\dagger) + \frac{i+ie^{i\Phi}}{2}(U\hat{b}_0 + V\hat{a}_0^\dagger) \quad (2)$$

$$\hat{b}_3 = \frac{1+e^{i\Phi}}{2i}(U\hat{a}_0 + V\hat{b}_0^\dagger) + \frac{1-e^{i\Phi}}{2}(U\hat{b}_0 + V\hat{a}_0^\dagger) \,. \quad (3)$$

Since we assume that modes $\hat{a}_0$ and $\hat{b}_0$ are in the vacuum state, two mode squeezed vacuum in modes $\hat{a}_1$ and $\hat{b}_1$ re-

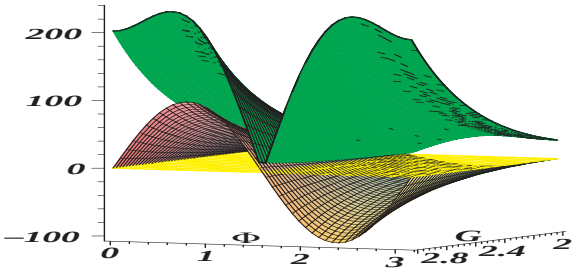

FIG. 2: Signal $\langle \hat{P} \rangle$ and the square root of the signals second moment $\langle \hat{P}^2 \rangle$, see eqns. (5) and (6), give us an idea of the behavior of the noise when measuring the homodyne current product (5).

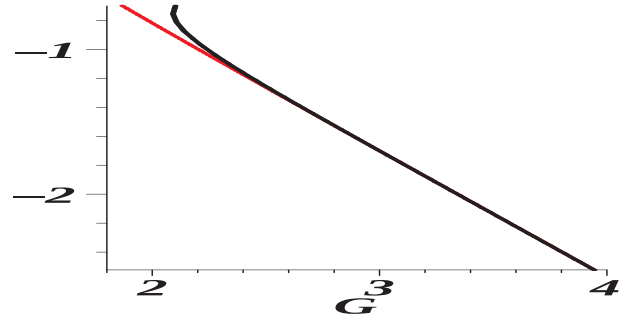

FIG. 3: Logarithmic plot of minimum phase spread $\log_{10}(\delta\varphi)$ as a function of the single pass gain G determined from (8) (curved black line) and of four times the inverse intensity $\log_{10}(4/(2\sinh(G)^2))$ (straight red line) confirming that $\delta\varphi = 4/(2\sinh(G)^2) = 4/\langle N \rangle$.

sults, parameterized by the squeezing or gain parameter G. The corresponding intensity $\langle N \rangle$ is [1]

$$\langle N \rangle \doteq \langle \hat{a}_3^\dagger \hat{a}_3 + \hat{b}_3^\dagger \hat{b}_3 \rangle = \langle \hat{a}_1^\dagger \hat{a}_1 + \hat{b}_1^\dagger \hat{b}_1 \rangle = 2\sinh(G)^2 \ . \quad (4)$$

It is well know that balanced homodyne detection measures the quadrature components of the monitored fields. We assume a relative phase of zero between local oscillator and our interferometric modes $\hat{a}_3$ and $\hat{b}_3$. In this case the photo currents of detectors A and B are proportional to the expectation values of $\hat{a}_3^\dagger + \hat{a}_3$ and $\hat{b}_3^\dagger + \hat{b}_3$ [1, 22]. The product P of the photo-currents is the signal we are interested in, it amounts to

$$\langle \hat{P} \rangle = \langle (\hat{a}_3^\dagger + \hat{a}_3)(\hat{b}_3^\dagger + \hat{b}_3) \rangle = \sinh(G)\cosh(G)\sin(2\Phi). \quad (5)$$

Note, that we observe a double period in the phase interval $\Phi = 0, ..., 2\pi$ in Eq. (5) and in FIG. 2 because our signal stems from the product of two homodyne currents. The corresponding second moment $\langle \hat{P}^2 \rangle$ is

$$\langle \hat{P}^2 \rangle = 1 + [\frac{7}{4} + \cos(2\Phi) - \frac{3}{4}\cos(4\Phi)] \left(\frac{\langle N \rangle^2}{2} + \langle N \rangle \right), \quad (6)$$

where we used the intensity expression (4). This yields the standard deviation $\sigma = \sqrt{\langle \hat{P}(\Phi)^2 \rangle - \langle \hat{P}(\Phi) \rangle^2}$

$$\sigma(\Phi) = \sqrt{\left(\frac{\langle N \rangle^2}{2} + \langle N \rangle \right) [\frac{3}{2} + \cos(2\Phi) - \frac{\cos(4\Phi)}{2}] + 1}, \quad (7)$$

which is minimal for $\Phi_{min} \doteq \phi = \pi/2$. Consequently the associated standard expression for the phase resolution limit $\delta\phi = \sigma(\Phi)/|\partial P/\partial\Phi|_{\Phi=\pi/2}$ is $1/|\partial P/\partial\Phi|_{\Phi=\phi} = 1/\sqrt{\langle N \rangle^2 + 2\langle N \rangle} \approx 1/\langle N \rangle$. This result seems to indicate that we can reach the Heisenberg limit since the minimal detected phase difference $\delta\phi \approx 1/\langle N \rangle$. But an inspection of the behavior of the second moment of the signal in FIG. 2 shows that the noise varies greatly in the vicinity of the optimal point $\phi = \pi/2$. We therefore have to analyze the behavior of the noise-valley around ϕ more closely. It turns out that the rapid growth of noise away from the optimal point does not let us achieve Heisenberg-limit resolution but the gradient of the slopes is sufficiently low to allow for a reduced phase resolution that *scales like* the Heisenberg limit, namely, according to our main result (1). Note, that a similar problem was encountered in reference [4] which was resolved by the stipulation that the interferometer acted 'phase-conjugated', meaning, when arm $\hat{a}_2$ lengthens $\hat{b}_2$ contracts by the same amount. In the present case this solution does not help and we have to accept a diminished performance. To derive our limit (1), let us remind ourselves of the standard derivation for the noise-induced phase-spread that limits interferometric resolution. Assuming that we encounter a noisy signal $P(\Phi) \pm \sigma(\Phi)$ with standard deviation σ we want to be able to tell the parameter ϕ apart from $\phi + \Delta\phi$. We therefore require (assuming, for definiteness, that $P \geq 0$ and growing with increasing Φ) that, according to the Rayleigh-criterion, $P(\phi) + \frac{\sigma(\phi)}{2} \lessapprox P(\phi + \Delta\phi) - \frac{\sigma(\phi+\Delta\phi)}{2}$. Approximating $P(\phi + \Delta\phi) \approx P(\phi) + \Delta\phi \cdot \partial P(\phi)/\partial\phi$, assuming equality of left and right hand side in order to determine the smallest permissible $\delta\phi$ and that the variance does not change appreciably $\sigma(\phi + \Delta\phi) \approx \sigma(\phi)$ this yields the standard expression for the phase resolution limit $\delta\phi = \sigma(\phi)/|\partial P/\partial\Phi|_{\Phi=\phi}$. In our case, however, we need to look at an expression which accounts for the changing variance; we therefore have to include both variances $\sigma(\varphi)$ and $\sigma(\varphi + \delta\varphi)$, according to the above discussion this leads to the modified criterion

$$\delta\varphi = \frac{\sigma(\varphi) + \sigma(\varphi + \delta\varphi)}{2} \cdot \frac{1}{|\partial P/\partial\Phi|_{\Phi=\varphi}} \ . \quad (8)$$

Choosing the optimal working point $\varphi = \pi/2$, this yields an implicit equation for $\delta\varphi$ which is not too easy to solve in the general case but for sufficiently high intensities ($G > 2.5 \hookrightarrow \langle N \rangle > 2\sinh(2.5)^2 \approx 73$ photons) we find $\delta\varphi = 4/\langle N \rangle$. This is illustrated by FIG. 3 and can be verified by direct substitution into (8). Because in our scheme the noise is phase sensitive it only works at particular phase settings (odd multiples of $\pi/2$, see FIG. 2) and our setup has to include a feedback mechanism – not

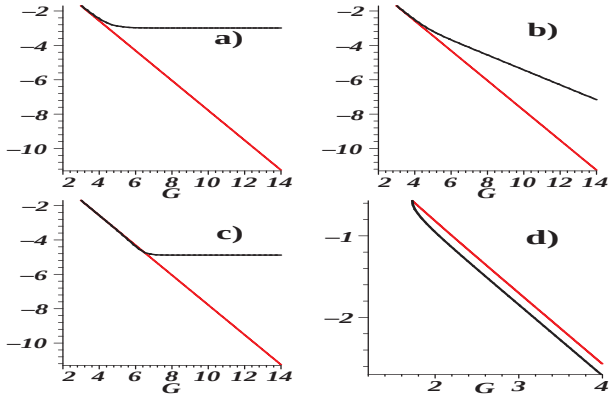

FIG. 4: Logarithmic plot of minimum phase spread $\log_{10}(\delta\varphi)$ determined from (8) (curved black lines) and of four times the inverse intensity $\log_{10}(4/(2\sinh(G)^2))$ (straight red lines) comparing various loss mechanisms: a) $\alpha_1 = \beta_1 = \pi/300$, b) $\alpha_2 = \beta_2 = \pi/300$, c) $\Delta_1 = 1/300000$, d) $\Delta_2 = -1/3$. Note the different orders of magnitude in the values of Δ_1 and Δ_2 and the fact that 'd)', surprisingly, shows a slight *improvement* in performance for a large negative imbalance $\Delta_2 = -1/3$.

mentioned in FIG. 1.

Robustness and further increase in sensitivity: Having shown that our scheme allows for Heisenberg-limit–like scaling in interferometric sensitivity we would also like to look at its sensitivity to experimental imperfections. Balanced homodyne detection amplifies quantum features to the classical level [1]. For strong fields detector losses can be kept small [18, 19, 22] and will therefore not be discussed further.

More importantly, losses and imbalances in the state preparation and interferometric part of the setup sketched in FIG. 1 deserve consideration. The main question we want to address is whether the introduction of experimental imperfections leads to a gradual loss of performance or whether we might be unlucky and a qualitative change in behavior results from any minute imperfection. It turns out that the former is the case, yet, experimental demands on the state preparation part of the setup are very high.

FIG. 4 compares the various cases for losses and imbalances and shows that the system is more forgiving for losses in the interferometer part than in the state preparation part: the utilized quantum state has to be prepared with great skill but the scheme is comparatively robust to imperfections of the interferometer. When all imperfections are studied simultaneously their effects add up, i.e., tend to be dominated by the largest effect(s).

Let us first consider losses in the state preparation part of the setup, i.e. losses in modes $\hat{a}_1$ and $\hat{b}_1$ extending from inside the crystal to the first beam-splitter B_1. They are described by the mode-transformations $\hat{a}_1 \mapsto \cos(\alpha_1)\hat{a}_1 + \sin(\alpha_1)\hat{u}_1$ and $\hat{b}_1 \mapsto \cos(\beta_1)\hat{b}_1 + \sin(\beta_1)\hat{v}_1$ plus subsequent tracing over the loss modes (not mentioned) and the admixed vacuum modes $\hat{u}_1$ and $\hat{v}_1$. It turns out that the qualitative picture does not depend much on the details such as whether the loss parameters α_1 and β_1 are equal or the losses occur in one channel only. Thus, with experiments in mind, let us assume symmetric losses, namely $\alpha_1 = \beta_1 = \pi/300 \approx 0.01$ leading to $0.0001 = 0.01$ % losses in both channels. For example, mode-mismatch at the beam splitter B_1 leads to such symmetrical admixture of vacuum. This scheme is very sensitive to losses in the state preparation part of the setup and shows saturation of performance, see FIG. 4 a): to gain an order of magnitude in performance α_1 and β_1 have to be decreased by half an order of magnitude, namely, $\delta\varphi$ saturates at about $9\alpha_1^2$.

Losses in the interferometric part of the setup (modes $\hat{a}_2$ and $\hat{b}_2$) are analogously described by loss parameters α_2 and β_2 which parameterize the admixture of two more vacuum modes $\hat{u}_2$ and $\hat{v}_2$ to the path modes $\hat{a}_2$ and $\hat{b}_2$. FIG. 4 b) illustrates the greater tolerance of our scheme to losses in the interferometer part of the setup. For the same loss values, $\alpha_2 = \beta_2 = \pi/300$ as for α_1 and β_1 before, the scheme shows a relatively better performance, indeed, the performance does not show saturation at all. Instead, at the threshold intensity $\approx 4/(9\alpha^2)$ it switches from $\delta\varphi \approx 4/\langle N\rangle$ to the poorer scaling $\delta\varphi = \kappa/\sqrt{\langle N\rangle}$, maintaining the ground it has gained. Namely, beyond the threshold intensity we find $\delta\varphi \approx 6\,|\alpha_2|/\sqrt{\langle N\rangle}$.

Analogously to the case of losses, the scheme is also much more sensitive to imbalances of the first beam-splitter B_1 than to those of B_2, which is described by

$$\hat{\mathsf{B}}_2 \begin{bmatrix} \hat{a}_2 \\ \hat{b}_2 \end{bmatrix} = \begin{bmatrix} -\cos(\frac{\pi}{4}+\Delta_2) & i\sin(\frac{\pi}{4}+\Delta_2) \\ -i\sin(\frac{\pi}{4}+\Delta_2) & \cos(\frac{\pi}{4}+\Delta_2) \end{bmatrix} \begin{bmatrix} \hat{a}_2 \\ \hat{b}_2 \end{bmatrix} \quad (9)$$

conforming with the case $\Delta_2 = 0$ used in the derivation of Eqs. (2) and (3). The imbalance in transformation $\hat{\mathsf{B}}_1$ is described, in full analogy, by an imbalance angle Δ_1. Similarly to the case of α_1 a non-zero Δ_1 leads to saturation: for positive imbalances the saturation level is $\delta\varphi \approx 4\Delta_1$ and it is $\delta\varphi \approx 12|\Delta_1|$ for negative Δ_1.

It turns out that variation of Δ_2 modifies the coefficient κ but not the scaling exponent in $\delta\varphi = \kappa/\langle N\rangle$; as mentioned above, for $\Delta_2 = 0$ we find $\delta\varphi = 4/\langle N\rangle$. Note that, surprisingly, a large (negative) imbalance Δ_2, as is displayed in FIG. 4 d), yields a small *increase* in performance quality (κ is being reduced). I cannot explain this finding and I think it deserves further investigation and might even lead to a trick to reduce the scaling reported here down to the Heisenberg-limit $\delta\varphi = 1/\langle N\rangle$. Variation of the value of the imbalance parameter Δ_2 *alone*, leads to an optimal value for the imbalance of approximately $\Delta_2 \approx -0.2375 \hat{=} -13.61^o$ and to our central result Eq. (1). This probably is the best our scheme can offer.

Over recent years a consensus has emerged that a sharp photon number distribution is needed to reach the Heisenberg-limit [11, 15, 16, 17]. It was therefore even concluded that the perceived need of a sub-poissonian photon number distribution renders the two-mode squeezed vacuum state unsuitable for interferometry because of its super-poissonian thermal photon num-

ber distribution [11, 16]; in the light of these claims our central result Eq. (1) is rather surprising.

Note, that we did not discuss a criterion for the power of the pump beam driving the parametric down-conversion source and of the power needed for the strong local oscillator fields necessary to perform the balanced homodyne measurements H_a and H_b, see FIG. 1. If this is included, the effective performance of our scheme could be reclassified as less efficient, yet, it remains a scheme with Heisenberg-limit–like scaling. The penalty to pay is not too large for large intensities because the local oscillator's shot-noise-to-signal-ratio diminishes with increasing signal strength thus yielding very accurate homodyning signals. In this context I would also like to mention that there are promising recent ideas for efficient and bright down-conversion sources [23].

Also note, that the considerations of this paper might turn out to be of importance for atom-beam interferometry [15] since four-wave mixing has been reported yielding correlated atom beams in states similar to the two-mode squeezed vacuum states discussed here [24].

Conclusions: We have found that bosonic two-mode squeezed states can be used in an interferometer to achieve phase resolution near the Heisenberg-limit, see Eq. (1). This only works at particular phase settings, the noise is phase sensitive and the setup therefore needs a feedback mechanism. The degrading influence of experimental imperfections is analyzed and it is shown that requirements on the state-preparation part of the setup are very stringent. On the other hand our scheme is more robust with respect to imperfections of the interferometer part of the setup and it does not suffer from single-photon detection problems because it relies on balanced homodyne-detection.

Acknowledgments

I wish to thank Janne Ruostekoski for reading of this manuscript.

[1] M. O. Scully and M. S. Zubairy, *Quantum Optics*, (Cambridge Univ. Press, Cambridge, 1997).
[2] C. M. Caves, Phys. Rev. Lett. **45**, 75 (1980).
[3] C. M. Caves, Phys. Rev. D **23**, 1693 (1981).
[4] R. S. Bondurant and J. H. Shapiro, Phys. Rev. D **30**, 2548 (1984).
[5] B. Yurke, S. L. McCall, and J. R. Klauder, Phys. Rev. A **33**, 4033 (1986).
[6] M. Xiao, L.-A. Wu, and H. J. Kimble, Phys. Rev. Lett. **59**, 278 (1987).
[7] P. Grangier, R. E. Slusher, B. Yurke, and A. LaPorta, Phys. Rev. Lett. **59**, 2153 (1987).
[8] M. J. Holland and K. Burnett, Phys. Rev. Lett. **71**, 1355 (1993).
[9] M. Hillery and L. Mlodinow, Phys. Rev. A **48**, 1548 (1993).
[10] J. Jacobson, G. Björk, I. Chuang, and Y. Yamamoto, Phys. Rev. Lett. **74**, 4835 (1995).
[11] B. C. Sanders and G. J. Milburn, Phys. Rev. Lett. **75**, 2944 (1995).
[12] Z. Y. Ou, Phys. Rev. Lett. **77**, 2352 (1996); Phys. Rev. A **55**, 2598 (1997).
[13] C. Brif and A. Mann, Phys. Rev. A **54**, 4505 (1996).
[14] T. Kim, O. Pfister, M. J. Holland, J. Noh, and J. L. Hall, Phys. Rev. A **57**, 4004 (1998).
[15] J. Dowling, Phys. Rev. A **57**, 4736 (1998).
[16] C. C. Gerry and A. Benmoussa, Phys. Rev. A **65**, 033822 (2002).
[17] J. Söderholm *et al.*, quant-ph/0204031.
[18] D. T. Smithey, M. Beck, M. G. Raymer, and A. Faridani, Phys. Rev. Lett. **70** 1244 (1993).
[19] D. T. Smithey, M. Beck, M. Belsley, and M. G. Raymer, Phys. Rev. Lett. **69**, 2650 (1992).
[20] A. Lamas-Linares, J. C. Howell, and D. Bouwmeester, Nature **412**, 887 (2001).
[21] G. S. Agarwal, R. W. Boyd, E. M. Nagasako, and S. J. Bentley, Phys. Rev. Lett. **86**, 1389 (2001).
[22] C. W. Gardiner and P. Zoller, *Quantum Noise*, (Springer, Berlin, 2000).
[23] A. De Rossi and V. Berger, Phys. Rev. Lett. **88**, 043901 (2002).
[24] J. M. Vogels, K. Xu, and W. Ketterle, Phys. Rev. Lett. **89**, 020401 (2002); L. Deng *et al.*, Nature (London) **398**, 218 (1999).